Published in final edited form as:

IEEE Trans Ultrason Ferroelectr Freq Control. 2015 September ; 62(9): 1662–1673. doi:10.1109/TUFFC.2015.007113.

Harmonic Motion Imaging for Abdominal Tumor Detection and High-intensity Focused Ultrasound Ablation Monitoring: A Feasibility Study in a Transgenic Mouse Model of Pancreatic Cancer

Hong Chen [Member, IEEE],
Department of Biomedical Engineering, Columbia University, New York, New York, USA.

Gary Y. Hou,
Department of Biomedical Engineering, Columbia University, New York, New York, USA.

Yang Han [Member, IEEE],
Department of Biomedical Engineering, Columbia University, New York, New York, USA.

Thomas Payen [Member, IEEE],
Department of Biomedical Engineering, Columbia University, New York, New York, USA.

Carmine F. Palermo,
Herbert Irving Comprehensive Cancer Center, Columbia University, New York, New York, USA.

Kenneth P. Olive, and
Herbert Irving Comprehensive Cancer Center, Columbia University, New York, New York, USA.

Elisa E. Konofagou [Member, IEEE]
Department of Biomedical Engineering and Department of Radiology, Columbia University, New York, New York, USA.

Abstract

Harmonic motion imaging (HMI) is a radiation force-based elasticity imaging technique that tracks oscillatory tissue displacements induced by sinusoidal ultrasonic radiation force to assess relative tissue stiffness. The objective of this study was to evaluate the feasibility of HMI in pancreatic tumor detection and high-intensity focused ultrasound (HIFU) treatment monitoring. The HMI system consisted of a focused ultrasound transducer, which generated sinusoidal radiation force to induce oscillatory tissue motion at 50 Hz, and a diagnostic ultrasound transducer, which detected the axial tissue displacements based on acquired radiofrequency signals using a 1D cross-correlation algorithm. For pancreatic tumor detection, HMI images were generated for pancreatic tumors in transgenic mice and normal pancreases in wild-type mice. The obtained HMI images showed a high contrast between normal and malignant pancreases with an average peak-to-peak HMI displacement ratio of 3.2. Histological analysis showed that no tissue damage was associated with HMI when it was used for the sole purpose of elasticity imaging. For pancreatic tumor ablation monitoring, the focused ultrasound transducer was operated with a

Address correspondence to: Dr. Elisa Konofagou, Department of Biomedical Engineering, Columbia University, 351 Engineering Terrace, mail code 8904, 1210 Amsterdam Avenue, New York, NY, USA, ek2191@columbia.edu, Tel: 212-342-0863.

higher acoustic power and longer pulse length than that used in tumor detection to simultaneously induce HIFU thermal ablation and oscillatory tissue displacements, allowing HMI monitoring without interrupting tumor ablation. HMI monitoring of HIFU ablation found significant decreases in the peak-to-peak HMI displacements before and after HIFU ablation with a reduction rate ranging from 15.8% to 57.0%. The formation of thermal lesions after HIFU exposure was confirmed by histological analysis. This study demonstrated the feasibility of HMI in abdominal tumor detection and HIFU ablation monitoring.

Index Terms

Radiation force-based elasticity imaging; ultrasound imaging; harmonic motion imaging; high-intensity focused ultrasound; pancreatic cancer; thermal ablation

I. INTRODUCTION

Pancreatic cancer is the fourth leading cause of cancer death with the worst prognosis of any major tumor type [1]. Pancreatic ductal adenocarcinoma (PDA) constitutes over 90% of pancreatic cancer cases. More than 80% of PDA patients are diagnosed at an advanced stage as there is no simple early detection method [2]. Because of the frequent delay in diagnosis, these patients are not suitable for surgical resection, which is the only potentially curative treatment. Non-operative therapies have been investigated for pancreatic tumor therapy, among which high-intensity focused ultrasound (HIFU) as an emerging technology holds great promise as a non-invasive, nonionizing, and localized tumor ablation method [3]. Preliminary clinical studies have shown that HIFU is safe and feasible for palliative treatment of patients with unresectable pancreatic cancer [4], [5]. However, the clinical applicability of HIFU for pancreatic cancer treatment is impeded by the lack of affordable and robust treatment guidance techniques. Here, guidance is interpreted in the broadest sense to include pretreatment planning, HIFU focus localization, real-time monitoring of treatment procedure, real-time feed-back control of exposure, and quantitative assessment of thermal lesions.

Currently, clinical HIFU treatment guidance use either magnet resonance imaging (MRI) or ultrasound imaging. MRI-guided focused ultrasound is capable of providing high resolution images for treatment targeting, temperature monitoring, and post-treatment visualization of the thermal lesion [6]. Despite its advantages, MRI is costly, lacks portability, and imposes complex electromagnetic compatibility issues. B-mode ultrasound has been another imaging technique used commonly in clinical practice for HIFU monitoring. It has permitted visualization of severe tumors for treatment targeting. However, it is challenging to perform ultrasound-guided HIFU in patients with tumors that cannot be easily detected by B-mode. Moreover, B-mode imaging based thermal ablation monitoring relies on the presence of hyperechoic signatures formed by the enhanced reflection from cavitation or boiling bubbles induced by HIFU, which is not a precise marker for thermal ablation [7]. Therefore, ultrasound-guided HIFU treatment requires an imaging technique that is reliable in both detecting tumors for treatment planning and monitoring thermal ablation for treatment monitoring.

Ultrasound elasticity imaging is a widely investigated technology that has great potential for tumor detection and HIFU lesion monitoring based on the distinctive mechanical properties of tumors and thermal lesions compared with healthy tissue and untreated tissue, respectively. All elasticity imaging techniques involve mechanical excitation of the tissue and tracking of the tissue response. The mechanical excitation can be provided by acoustic radiation force, external excitation (i.e. elastography, sonoelasticity, transient elastography, magnetic resonance elastography (MRE)), or internal physiologic motion (i.e. cardiac strain imaging). Radiation force-based elasticity imaging methods remotely interrogate tissue mechanical properties by generating impulsive radiation force (i.e. acoustic radiation force impulse imaging (ARFI), spatially modulated ultrasound radiation force (SMURF), shear wave elasticity imaging (SWEI), supersonic shear imaging (SSI), shear wave spectroscopy, comb-push ultrasound shear elastography (CUSE)), or harmonic radiation force (i.e. vibro-acoustography, shear wave dispersion ultrasound vibrometry (SDUV), crawling wave sonography (CWS), and harmonic motion imaging (HMI)) [8]. HMI, the focus of this study, assesses relative tissue stiffness by tracking oscillatory tissue displacements (i.e., sinusoidal displacements at a specific frequency) induced by sinusoidal radiation force (i.e., harmonic radiation force) [9]. HMI uses two confocally-aligned ultrasound transducers: one focused ultrasound transducer driven by an amplitude-modulated continuous pulse for generating the sinusoidal radiation force within its focal zone and the other diagnostic imaging transducer for detecting the induced oscillatory tissue displacements. In general, the amplitudes of the oscillatory tissue displacements are inversely proportional to the tissue stiffness and thus provide qualitative estimation of tissue stiffness within the focal region.

Similar to many other elasticity imaging techniques, HMI can be used for both tumor detection and HIFU treatment monitoring; however, it has three unique advantages. First, the estimation of radiation force-induced small displacements is often interfered by various noise generated by physiologic motion, such as breathing, blood flow, and digestive tract movements. HMI shares the same advantage as other methods that employ harmonic radiation forces (e.g. vibro-acoustography, SDUV, and CWS) to induce an oscillatory tissue motion, allowing efficient reduction of those noises in displacement estimation as their frequencies are distinct from the oscillatory tissue motion frequency [10]. For HIFU monitoring, the oscillatory tissue motion also allows separation of tissue mechanical property changes from speed of sounds changes, as the latter introduces a linear shift in the HMI displacement in time, which can be easily separated from oscillatory tissue motion [11]. Second, the FUS transducer can be operated for the sole purpose of elasticity imaging without causing thermal ablation; meanwhile, it can also be operated at HIFU regimes, allowing simultaneous HIFU thermal ablation and ablation monitoring without stopping the HIFU treatment. For the sole purpose of elasticity imaging, the need of two transducers is a disadvantage of HMI; however, the FUS transducer can be a separated add-on system to be used with any standard clinical scanner for HMI, while other radiation-force based elasticity imaging techniques that use a single transducer require customized ultrasound scanners. Third, HMI uses a FUS transducer to generate the radiation force, while most other radiation force-based techniques use a diagnostic ultrasound probe to generate the radiation force. The radiation force generated by the FUS transducer can be much higher than that generated by an imaging probe. It is beneficial for inducing detectable displacements in deep-lying, stiff

abdominal tumors, such as the PDA. PDA is known to be a firm mass because of the presence of a dense collagenous stroma by desmoplastic reaction [12]. The use of the FUS transducer to generate the radiation force is especially important for inducing detectable displacements in HIFU-ablated tumors, which normally has even increased stiffness relative to tumors before HIFU ablation. Because of these unique advantages, HMI has great potential in pancreatic tumor detection and HIFU treatment monitoring.

For pancreatic tumor detection, both endoscopic and transabdominal ultrasound elasticity imaging techniques have been used in clinical studies as new approaches for evaluating pancreatic diseases based on the elasticity of pancreases. Endoscopic ultrasonography elastography is nowadays the most frequently used approach for elastographic examination of the pancreas [13]; however, it is minimally invasive and requires anesthesia, which limits its application only to selected patient population. Currently, ARFI and SWEI methods have been implemented on Siemens Acuson ultrasound scanner as Virtual Touch Tissue Imaging and Virtual Touch Tissue Quantification, respectively [8]. Both techniques have been demonstrated useful for diagnosing pancreatic tumor, pancreatic fibrosis, and pancreatitis [14]–[17]. Although non-invasive, making these two methods appropriate for screening asymptomatic patients, their successful application in the abdominal organs faces a unique challenge: they are sensitive to physiologic motion [14]. Harmonic radiation force-based elasticity imaging methods, such as HMI, can be more robust to physiologic motion as they use harmonic radiation force excitation at a specific frequency, which allows effective isolation of the acoustic radiation force induced tissue displacements from physiologic motion in the imaging plane.

For HIFU treatment monitoring, several elasticity imaging techniques have been developed for monitoring changes in tissue elasticity during HIFU treatment, including MRE [18], ultrasound quasi-static elastography [19][20], SSI [21]–[23], ARFI [24][25], and HMI [26] [10]. MRE has been proven to be feasible for assessing HIFU-induced thermal lesions [18]; however, it has the limitations of MRI, as mentioned before. Among all the ultrasound-based elasticity imaging techniques, quasi-static elastography is so far the only technique applied in human patients for HIFU monitoring. It used a balloon attached to a transrectal probe to apply static compression to prostates for visualizing HIFU lesions formed in prostate [27]. The application of this technique is limited to superficial targets of interest because the balloon needs to be in direct contact with the targets to generate sufficient compression for elastography. Moreover, the HIFU treatment needs to be stopped for tissue compression, which significantly increases the treatment duration. Radiation force-based imaging techniques, including ARFI, SSI and HMI, use remote tissue interrogation instead of direct compression. For the application of ARFI in HIFU monitoring, Bing et al. demonstrated the feasibility of using a diagnostic ultrasound system operated using a customized beam sequence to ablate *ex vivo* liver and monitor the resulting tissue stiffening using ARFI. Later, Lizzi *et al.* utilized short radiation force impulses generated by a HIFU transducer to induce tissue displacements without causing significant tissue heating and used another imaging probe to detect the displacements for tissue stiffness assessment at intervals during HIFU exposures. For the application of SSI in HIFU monitoring, Bercoff *et al.* proposed the use of SSI to detect and quantify the hardness of HIFU-induced lesions after

HIFU ablation. Arnal *et al.* tested the feasibility of SSI for real-time HIFU therapy monitoring *in vivo* on sheep muscle. SSI is capable of extracting quantitative tissue elasticity estimates, as the speed of a shear wave is proportional to the tissue shear modulus. Nevertheless, both SSI and ARFI require HIFU treatment to be turned off during imaging, which significantly increases the treatment duration and reduces the efficiency of an already lengthy HIFU treatment procedure. Moreover, both techniques have not been tested in tumors *in vivo.*

Because of the unique advantages of HMI in tumor detection and HIFU monitoring, it has become the only radiation force-based imaging technique that has been proved feasible for *in vivo* HIFU tumor ablation monitoring [10], [26]. Curiel *et al.* [26] investigated the feasibility of a 1D HMI system in monitoring and controlling HIFU ablation of subcutaneously implanted VX2 tumors in rabbits. They found that significant decreases in tissue displacement amplitudes could be used to validate tissue coagulation and control HIFU treatment. Maleke *et al.* [10] demonstrated the feasibility of a 2D HMI system with a phased array imaging probe for monitoring HIFU breast tumor therapy using a transgenic breast cancer mouse model. However, no study has been performed using HMI in HIFU ablation monitoring of abdominal tumors, such as pancreatic tumors.

This study aimed at evaluating the feasibility of HMI in pancreatic tumor detection and HIFU ablation monitoring using a transgenic mouse model of PDA that closely mimic human PDA. The feasibility of HMI in pancreatic tumor detection was assessed by comparing the peak-to-peak HMI displacements of pancreatic tumors with normal pancreases. The feasibility of HMI in pancreatic tumor HIFU ablation monitoring was evaluated by estimating peak-to-peak HMI displacement changes in pancreatic tumors during HIFU ablation. The results demonstrated the potential of HMI as an elasticity imaging technique in providing guidance for HIFU ablation of abdominal tumors.

II. MATERIALS AND METHODS

A. Experimental Setup

A schematic illustration of the main components of the HMI system is shown in Fig. 1a. 1D and 2D HMI systems were used in this study. Both systems can be used for tumor detection and HIFU treatment monitoring. In this study, the 1D system was used for pancreatic tumor detection, because the 1D system comprising of a 7.5 MHz single-element pulse-echo transducer provided higher spatial resolution than the 2D HMI system comprising of a 2.5 MHz phased-array imaging transducer. While, the 2D HMI system was used for pancreatic tumor HIFU treatment monitoring to provide a 2D view of the HIFU targeted region. A brief description of these two systems is as follows. For more details, please refer to our group's previous publications [28][29].

The 1D HMI system comprised of a single-element FUS transducer (center frequency = 4.755 MHz, Riverside Research Institute, New York, NY) and the 7.5 MHz single-element pulse-echo transducer (Olympus-NDT, Waltham, MA, USA) (Fig.1b). The FUS transducer was driven by amplitude-modulated sinusoidal signals generated by a dual-channel arbitrary waveform generator (AT33522A, Agilent Technologies Inc. Santa Clara, CA, USA) and

amplified by a nominal 50-dB gain power amplifier (325LA, E&I, Rochester, NY, USA). The pulse-echo transducer was confocally aligned through a hole in the center of the FUS transducer. The pulse-echo transducer was operated at a pulse repetition frequency (PRF) of 1 KHz using a pulser/receiver (Olympus-NDT, Waltham, MA, USA). The received radiofrequency (RF) signals from the pulser/receiver were filtered by a band-pass filter (Reactel Inc., Gaithersburg, Maryland, USA) with cutoff frequencies of f_{c1} = 5.84 MHz and f_{c2} = 8.66 MHz to remove the interference of the FUS beams and then recorded by a digitizer (Gage applied, Lockport, IL, USA) at a sampling frequency of 100 MHz. For the synchronization of RF signal acquisition and FUS exposure, the digitizer was triggered by the function generator's sync signals. The coupled transducer pair was mounted onto a 3D positioning system (Velmex Inc., Bloomfield, NY, USA).

The 2D HMI system consisted of a 93-element FUS phase array transducer (center frequency=4.5 MHz; H-178, Sonic Concept Inc. Bothell WA, USA) and a 64-element phase array imaging probe (center frequency = 2.5 MHz, P4-2, ATL, Bothell, WA, USA) (Fig.1c). In this feasibility study, the 93 elements of the FUS transducer were driven in phase using the same function generator and power amplifier as the 1D system; thus, no electronic steering of the FUS focus was employed. The imaging probe was inserted through the hole in the center of the FUS transducer and confocally aligned with it. The imaging probe was operated by a research ultrasound imaging system (V1, Verasonics, Bothell, WA, USA). For the synchronization of the data acquisition by the Verasonics system and the FUS exposure, the FUS transducer was simultaneously triggered by the Verasonics system.

B. Animal experiment protocol

In accordance with the National Institutes of Health Guidelines for animal research, all animal procedures were reviewed and approved by the Institutional Animal Care and Use Committee of the Columbia University. The animal model used was a transgenic mouse model of PDA, K-ras$^{LSL.G12D/+}$; p53$^{R172H/+}$; PdxCre (KPC) mice [30], [31]. The KPC mice develop pancreatic tumors with pathophysiological and molecular features resembling those of human PDA [30]. In addition, as the KPC mice enrolled in our study were all at the late stage of their lives (their tumor diameters were larger than 5 mm), the pancreatic tumors could spread to the whole pancreas; therefore, wild-type mice (strain: C57BL/6, age: 6-8 weeks, Harlan Sprague Dawley, Indianapolis, IN, USA) were used as the healthy control in the pancreatic tumor detection study.

During the whole procedure, mice were anesthetized with 1~2% isoflurane in oxygen. They were placed supine on a heating pad. Their abdomen was depilated using depilatory cream and cleaned. Then, a water container filled with degassed water was placed on the abdomen and coupled with degassed ultrasound gel (Fig.1a). The bottom of the water container had a window sealed with an almost acoustically and optically transparent membrane (Tegaderm™, St. Paul, MN, USA).

In order to precisely locate the pancreas, a high-frequency ultrasound imaging system (Vevo 770, VisualSonics Inc. Toronto, Canada) coupled with a high-frequency ultrasound probe (RMV-707B) of a nominal center frequency of 30 MHz was used. The Vevo probe was attached to the 3D positioning system shown in Fig. 1a. The mouse abdomen was then

scanned by the Vevo system using B-mode imaging to find pancreatic tumors in the KPC mice or normal pancreases in the wild-type mice. Under the guidance of the Vevo system, a grid was then placed in the water container above the mouse and adjusted so that the node on the grid was directly above the targeted tumor location. The Vevo probe was then replaced by either the 1D or 2D HMI transducer pair, consisting of the confocally aligned FUS transducer and imaging probe. The imaging probe of the HMI transducer pair was then used to align the focus of the HMI transducer pair to the node on the grid. For the 1D HMI system, raster scan of the grid by the pulse-echo transducer was performed to locate the node, which was similar to the technique our group developed before [32]. For the 2D HMI system, B-mode images acquired with the HMI imaging probe were used to locate the node. The height of the HMI transducer pair was subsequently adjusted so that its focus was within the tumor. Here, we note that the 2D HMI imaging probe was capable of identifying the location of the tumor when the tumor size was sufficiently large; however, its resolution was insufficient for unequivocally outlining the boundary of the tumor, thus the Vevo system was used to assist with tumor targeting.

C. HMI Data Acquisition

The feasibility of HMI in pancreatic tumor detection was evaluated using the 1D HMI system by comparing the peak-to-peak HMI displacements of pancreatic tumors in the KPC mice (n=3) and normal pancreases in wild-type mice (n=3). To form 2D HMI images using the 1D HMI system, the focal point of the HMI transducer pair was moved across a transverse plane with a width of 10 mm in a point-by-point raster scan pattern with a step size of 0.25 mm. At each spot, the FUS exposure was 200-ms long, during which 200 A-mode RF lines at 1 kHz pulse repetition frequency (PRF) were acquired at a sampling frequency of 100 MHz. With such high PRF, de-correlation in displacement estimation can be minimized. The FUS acoustic power measured in water was 5.04 W. The 200-ms FUS exposure induced 10-cycle tissue oscillations at 50 Hz. In each mouse, parallel transverse planes with 1 or 2 mm apart were scanned using the 1D HMI system. The main 1D HMI system parameters are summarized in Table 1.

A total of 6 KPC mice were enrolled for HIFU ablation monitoring. Guided by Vevo B-mode images, 1-3 HIFU targeted locations were selected in each tumor at regions where there were no intestine and stomach in the acoustic path to ensure no obstruction of HIFU beam by bowel gas. One mouse without such acoustic window was excluded from the data analysis. The 2D HMI system was used for HIFU ablation monitoring. The FUS transducer was operated to induce HIFU thermal ablation and oscillatory tissue displacements at the same time, allowing HMI monitoring without interrupting tumor ablation. Prior to HIFU ablation, a standard B-mode image of the targeted region was acquired using the HMI imaging probe. Then, HIFU with an acoustic power output of 7.56 W in water was applied for 120 s. Previous studies by our group demonstrated that same HIFU treatment protocol consistently generated thermal lesions by slow denaturation without producing extensive boiling effects in *ex vivo* canine livers and HMI detected significant decreases in HMI displacement amplitudes before and after HIFU ablation [28]. Because HMI did not interrupt HIFU ablation, HIFU sonication was operated with a duty cycle of 100%. A custom ultra-fast flash imaging sequence for the 64-element phase array imaging probe (64-

element for transmit and 64-element for receive) was developed using the Verasonics platform. A GPU-based sparse-matrix algorithm was used for fast beamforming [29]. About every 3 s during HIFU exposure, 200 beamformed frames at a frame rate of 1 kHz were acquired during 200-ms HIFU exposure. Same as the 1D HMI system, the 200-ms HIFU exposure induced 10-cycle tissue oscillations at 50 Hz. Here we note that although the 200 image frames were acquired every 3 seconds, the HIFU exposure was continuous without interruption. A linear interpolation technique was used to upsample the RF signals by a factor of 8 (a factor chosen to improve precision in displacement estimation) before saving to the host computer, achieving a sampling frequency of 80 MHz. The main 2D HMI system parameters are summarized in Table 1.

D. HMI Displacement Estimation

The main signal post-processing techniques were similar for the 1D and 2D HMI systems (Fig.2). Each set of the 200 RF lines acquired using the 1D HMI system at each raster scanning location during 200-ms FUS exposure was processed together. Similarly, each set of the 200 RF frames acquired at each time point using the 2D HMI system during 200-ms HIFU exposure was processed together. Again, the 200-ms exposure induced 10-cycle tissue oscillations at 50 Hz. The processing methods were as follows: First, the interference of the FUS beam in the received RF signals was removed. For the 1D HMI processing, the interference of the FUS beam was removed by the analog band-pass filter as described previously. For the 2D HMI processing, it was achieved by digital low-pass filtering (f_{cutoff}=4 MHz) during post-processing (Figs. 2b and 2c). Second, the incremental axial tissue displacements were estimated by performing a fast 1D normalized cross-correlation between sequentially acquired tracking lines [33] (Figs. 2d and 2e). The RF window size was equal to 10 wavelengths of the imaging probe and the window overlap was 95%. Third, a linear bandpass filter with cutoff frequencies of f_{c1}=30 Hz and f_{c2}=70 Hz was applied to the estimated displacements along the temporal space to extract oscillatory tissue motion at 50 Hz (Figs. 2f and 2g). It reduced lower frequency noise stemming from breathing, blood flow, and digestive tract movements, as well as higher frequency jitter in displacement estimation. A threshold on the cross-correlation coefficient ($r > 0.9$) was applied to eliminate poor displacement estimates mainly in the coupling water. Fourth, the mean peak-to-peak HMI displacement and standard deviation of the 10-cycle oscillations at 50 Hz were calculated. Lastly, the aforementioned processing was repeated at each raster scan point to reconstruct the 2D HMI images for pancreatic tumor detection or repeated at each HIFU ablation time point to obtain HMI images for HIFU treatment monitoring.

For pancreatic tumor detection, the outlines of the pancreatic tumor and normal pancreas were manually delineated on the Vevo B-mode images by a trained observer without knowledge of the location and ultrasound parameters of each sonication. These outlines were applied to the corresponding HMI images. The mean and standard deviation of the peak-to-peak HMI displacement within each outlined region were calculated for each scanning plane. Finally, the mean HMI displacements calculated from three parallel scanning planes were averaged to obtain the final HMI displacement for each mouse.

For pancreatic tumor HIFU ablation monitoring, we first identified the point with the maximum displacement at the beginning of HIFU ablation (t=0 s). At that point, the mean and standard deviation of the peak-to-peak HMI displacement calculated based on the 200 RF frames acquired at each time point were obtained for the whole HIFU ablation process. The percentage of HMI displacement changes at the end of HIFU ablation (t=117 s) over the initial displacement (t=0 s) was calculated.

An unpaired two-tailed student's t-test using GraphPad Prism (Version 5.01, La Jolla, CA, USA) was used to compare between the peak-to-peak displacement amplitudes of pancreatic tumors and normal pancreases. The same test was also used to compare HMI displacement amplitudes of pancreatic tumors at the beginning of HIFU ablation (t = 0 s) and at the end of HIFU ablation (t = 117 s). A *P* value of 0.05 was considered to represent a significant difference.

E. Histological Analysis

All mice were sacrificed immediately after the previously described procedure. Pancreatic tumors in the transgenic mice and normal pancreases in the wild-type mice were harvested for histological evaluation. The excised tissue was first fixed in 4% paraformaldehyde. After post-fixation processing, tissue was paraffin embedded, sectioned, and stained with hematoxylin and eosin (H&E). Bright-field microscopy images of the stained sections were acquired and evaluated by a blinded, trained expert.

III. RESULTS

A. HMI for Pancreatic Imaging

A representative HMI image of the normal pancreas is shown in Fig. 3a. The location of the pancreas, as well as the liver and kidney in its close proximate, was outlined based on the corresponding Vevo B-mode image obtained at approximately the same imaging plane (Fig. 3b). The peak-to-peak HMI displacements of the normal pancreas, liver and kidney averaged within the outlined regions were 19.9±1.8, 17.0±2.2 and 12.2±4.1 μm (mean ± standard deviation), respectively. Fig. 3c shows one example of the HMI image of a pancreatic tumor. The tumor was confirmed by the corresponding Vevo B-mode image (Fig. 3d). The peak-to-peak HMI displacement of the pancreatic tumor within the outlined region was 5.2±0.8 μm (mean ± standard deviation), which was significantly lower than that of the normal pancreas.

When comparing the peak-to-peak HMI displacements of normal pancreases in the control group and pancreatic tumors in the KPC mouse group, a statistically significant difference was found, as shown in Fig. 4a. The average peak-to-peak displacement of normal pancreases (18.0±1.7 μm) was 3.2 times higher than that of pancreatic tumors (5.6±0.9 μm). Histological analysis found no tissue damage in normal pancreases and pancreatic tumors. Figs. 4b and 4c show representative H&E stained images from a pancreatic tumor without performing HMI and a pancreatic tumor after performing HMI, respectively. No signs of tissue damage were found in Fig. 4c.

B. HMI for Pancreatic Tumor HIFU Ablation Monitoring

Figs. 5b-f show peak-to-peak HMI displacement images obtained at different time points during HIFU ablation. Fig. 5a presents the B-mode image acquired before HIFU ablation using the same HMI imaging probe at the same imaging plane, in which the locations of the membrane at the bottom of the water container, the mouse, and the tumor are highlighted. The tumor boundary was drawn in reference to the corresponding Vevo B-mode image. At HIFU exposure time t = 0 s (Fig. 5b), the HMI image clearly shows the location of the HIFU focal region, where the peak-to-peak HMI displacement was higher than all other regions. It shows that the HIFU focal region was precisely targeted within the tumor. Figs. 5b-f exhibit that the HMI displacements within the focal region decreased over time.

Figs. 6a and 6b present the mean and standard deviation of the peak-to-peak HMI displacement over the whole HIFU ablation process at the point with the highest displacement at t = 0 s for two representative cases. Fig. 6a displays the displacement curve for the case shown in Fig. 5. These two curves representatively show two distinct trends in tissue displacement change during HIFU ablation. Fig. 6a shows a trend of displacement decrease over time, suggesting tissue stiffening during HIFU ablation. Figs. 6b exhibits a displacement increase and then decrease, denoting tissue softening followed by stiffening during HIFU ablation. Nevertheless, both figures present a consistent reduction in the HMI displacement amplitudes at the end of the HIFU ablation (t = 117 s) when compared with those at the beginning of HIFU ablation (t = 0 s) with a reduction rate of 24.4% and 31.5%, respectively (Fig. 6d).

A summary of the mean and standard deviation of the peak-to-peak HMI displacement before and after HIFU ablation for 5 KPC mice at 11 HIFU exposure locations is shown in Fig. 7c. Signification decreases (t-test, $p<0.05$) in the HMI displacement amplitudes after HIFU ablation were observed in all locations (Fig. 6c). Fig. 6d shows that all locations had a consistent reduction in HMI displacement at the end of HIFU ablation when compared with those at the beginning of HIFU ablation with a reduction percentage ranged from 15.8% to 57.0%. The H&E staining results confirmed that thermal lesions were generated in the 5 mice and representative images from two mice are shown in Figs.7(b) and 7(c).

IV. DISCUSSION

The clinical application of ultrasound-guided HIFU in tumor ablation is currently limited by the lack of reliable ultrasound imaging techniques for HIFU treatment guidance. This study demonstrated for the first time the feasibility of HMI in pancreatic tumor detection and HIFU ablation monitoring using a transgenic mouse model of PDA that closely recapitulates human disease.

This study demonstrated that HMI was capable of detecting pancreatic tumors in a mouse model *in vivo*. It was found that the peak-to-peak HMI displacement of the pancreatic tumor was on the average 3.2 times lower than that of the normal pancreas. Although tissue elasticity cannot be directly quantified, this displacement contrast ratio still serves as an insightful qualitative indicator for comparing the stiffness of different types of tissues, considering that the applied radiation force was approximately at a similar level. In addition,

HMI can also image other abdominal organs besides the pancreas, such as the liver and kidney, as shown in Fig. 3a. Histological analysis showed that when HMI was used for the sole purpose of elasticity imaging, no tissue damage was found. The feasibility of HMI in tissue stiffness detection has been demonstrated *in vitro*, *ex vivo* and *in vivo* [10], [11], [26], [34]–[38]; however, for the first time, we demonstrated its feasibility in imaging a deep-lying, stiff, moving abdominal tumor in mice.

Moreover, this study demonstrated that HMI is feasible for monitoring HIFU ablation of pancreatic tumors in a transgenic mouse model. HMI monitoring was performed during HIFU ablation, without interrupting HIFU treatment. It can be used for HIFU beam localization for treatment targeting. As shown in Fig. 5b, we can clearly identify the HIFU targeted region, where the HMI displacement amplitudes were higher than other regions. Two different trends in tissue stiffness change during HIFU ablation were observed: stiffening only (Fig. 6a) and softening-then-stiffening (Fig. 6b). We speculate that these different trends were associated with the underlying structural differences at different targeted locations [29], [37]. Statistic significant decreases in the peak-to-peak HMI displacements were obtained in all HIFU exposures (Fig. 6c) with decrease percentages ranged from 15.8% to 57.0% (Fig.6d). The formation of thermal lesions in all HIFU ablated mice was confirmed by histological analysis (Fig. 7).

In summary, HMI, as a radiation force-based elasticity imaging technique, provides a robust HIFU treatment guidance technique. A primary determinant of the radiation force-based elasticity image quality is the separation of the acoustic radiation force-induced small tissue displacements from any physiologic motion, such as breathing, blood flow, and digestive tract movements. Physiologic motion filtering is challenging for other impulsive radiation force-based imaging techniques, such as ARFI, SWEI, and SSI, because of significant spectrum overlap between the slow radiation force-induced tissue motion and physiologic motion. HMI uses harmonic radiation force to induce oscillatory tissue displacements at a specific known frequency, which allows efficient reduction of noise generated by physiologic motion in displacement estimation. In a previous publication [10], our group demonstrated that HMI was not affected by respiratory motion of mice. In the present study, Figs. 2f and 2g further illustrate that the use of a band-pass filter can filter out the oscillatory tissue motion from lower frequency tissue motions or higher frequency jitter, which renders HMI more robust to physiologic motion induced artifacts than impulsive radiation force imaging techniques. Moreover, for monitoring pancreatic tumor HIFU ablation using radiation force-based elasticity imaging, a great challenge is the ability to induce detectable displacement at depth in a stiff tumor. Different from many other tumors, PDA is characterized by the formation of stiff scar tissue by desmoplastic reaction. The use of the HIFU transducer to generate the radiation force, instead of using the imaging probe as in many other radiation force-based techniques, is beneficial for inducing detectable displacements in deep-seated stiff pancreatic tumors and especially thermally ablated pancreatic tumors, which has an even higher stiffness than that before ablation. In addition, HMI as used here estimated and imaged the resulting tissue displacements and assumed that the radiation force focused into a focal region of a few millimeters was uniformly applied within the focal region. As a result, the displacements estimated are inversely proportional to

the underlying stiffness. Although not the focus of this study, our group demonstrated that the underlying tissue elasticity can be obtained from HMI either with [35] or without [39] shear waves.

This study has several limitations. First, as mentioned earlier, HMI induces oscillatory tissue motion at a specific low-frequency, allowing efficient reduction of noises from sources such as respiratory motion. Respiration-induced movement of the pancreas in the abdomen can degrade the spatial registration of HMI. For mice under anesthesia, the respiration-induced motion of the pancreas was at a small magnitude [10]; however, this motion has to be taken into consideration for future clinical applications as the human pancreas moves up to ~20 mm during respiration [40]. In the future, ultrasound-based motion tracking technique will be developed to compensate pancreas movement in order to achieve consistent spatial registration in HMI. Moreover, the imaging probe used in the 2D system had a center frequency of 2.5 MHz, which was optimized to achieve deeper penetration in future clinical applications. A higher frequency imaging probe will be used in the future for small animal studies to achieve higher spatial resolution in HMI. The use of the higher frequency probe will also allow us to perform tumor targeting without the assistance of the Vevo system. Furthermore, relative low-energy HIFU with long exposure time was used in the present study to induce slow tissue denaturation. Our group has demonstrated the feasibility of HMI in monitoring high-energy HIFU treatment with tissue boiling in *ex vivo* tissue [37][28]. Future studies will explore the feasibility of *in vivo* HMI monitoring for HIFU treatment with boiling. In addition, HMI clearly located the HIFU focal region and monitored the stiffness changes of that region over time. However, because of the difficulty involved in sectioning through the excised pancreas to align with the imaging plane of the HMI, precise quantitative comparisons of actual lesion sizes and HMI images was not conclusive. To assess the thermal lesion sizes based on the HMI images, further effort is needed to spatially register the HMI images with histological images in order to provide information such as the onset of lesion formation and lesion sizes. Future study will also look into the correlation between tissue structures and the trends of HMI displacement changes to better understand tissue mechanical responses during HIFU ablation. The current study laid the foundations for future development of HMI as an imaging technique for ultrasound-guided HIFU treatment with the ability to detect tumors for treatment planning, evaluate tissue stiffness change during HIFU ablation for on-line treatment monitoring and feed-back control of exposure, and assess thermal lesion sizes for treatment evaluation.

V. CONCLUSION

This study demonstrated the feasibility of HMI in pancreatic tumor detection and HIFU ablation monitoring using a transgenic mouse model of PDA that closely recapitulates human disease. HMI uses one FUS transducer driven by an amplitude-modulated continuous pulse for generating sinusoidal radiation force and the other diagnostic imaging transducer for detecting the induced oscillatory tissue displacements. For pancreatic tumor detection, the FUS transducer was operated for the sole purpose of elasticity imaging. 2D HMI images of pancreatic tumors and normal pancreases were generated. The peak-to-peak HMI displacements of normal pancreases were on the average 3.2 times higher than those of the pancreatic tumors. Histology analysis showed that no tissue damage was associated with

HMI when used for the sole purpose of elasticity imaging. For HIFU ablation monitoring, the FUS transducer was operated at HIFU regime to induce thermal ablation and simultaneously generate sinusoidal radiation force for ablation monitoring. HMI monitoring of HIFU ablation showed consistent tissue stiffening after 2-min HIFU exposure. The peak-to-peak HMI displacements at the end of HIFU ablation decreased by 15.8% to 57.0% from the initial displacements. The formation of thermal lesions was confirmed by histological staining. This study validated the feasibility of HMI for pancreatic tumor detection and HIFU ablation monitoring, which constitutes an important step toward future clinical applications of HMI as a promising imaging technique for HIFU treatment guidance.

Acknowledgments

Financial support: This work was supported by the National Institutes of Health under grant R01EB014496 and Lustgarten Foundation for Pancreatic Cancer Research.

REFERENCES

1. Siegel R. Cancer statistics, 2013. CA Cancer J. Clin. 2013; 63(1):11–30. [PubMed: 23335087]
2. Klein AP. Identifying people at a high risk of developing pancreatic cancer. Nat. Rev. Cancer. Jan; 2013 13(1):66–74. [PubMed: 23222481]
3. Khokhlova TD, Hwang JH. HIFU for palliative treatment of pancreatic cancer. J. Gastrointest. Oncol. Sep; 2011 2(3):175–184. [PubMed: 22811848]
4. Wu F, et al. Feasibility of US-guided high-intensity focused ultrasound treatment in patients with advanced pancreatic cancer: initial experience. Radiology. Sep; 2005 236(3):1034–1040. [PubMed: 16055692]
5. Anzidei M, et al. Magnetic resonance-guided focused ultrasound ablation in abdominal moving organs: a feasibility study in selected cases of pancreatic and liver cancer. Cardiovasc. Intervent. Radiol. Mar.2014 :1–7.
6. Hynynen K. MRI-guided focused ultrasound treatments. Ultrasonics. 2010; 50(2):221–229. [PubMed: 19818981]
7. Goldberg S, Grassi C. Image-guided tumor ablation: standardization of terminology and reporting criteria. Radiology. 2009; (1)
8. Doherty JR, Trahey GE, Nightingale KR, Palmeri ML. Acoustic radiation force elasticity imaging in diagnostic ultrasound. IEEE Trans. Ultrason. Ferroelectr. Freq. Control. Apr; 2013 60(4):685–701. [PubMed: 23549529]
9. Konofagou EE, Maleke C, Vappou J. Harmonic Motion Imaging for Tumor Imaging and Treatment Monitoring. Soft Tissue Biomechanical Modeling for Computer Assisted Surgery. 2012:257–280.
10. Maleke C, Konofagou EE. In vivo feasibility of real-time monitoring of focused ultrasound surgery (FUS) using harmonic motion imaging (HMI). IEEE Trans. Biomed. Eng. Jan; 2010 57(1):7–11. [PubMed: 19643703]
11. Maleke C, Pernot M, Konofagou EE. Single-Element Focused Ultrasound Transducer Method for Harmonic Motion Imaging. Ultrason. Imaging. Jul; 2006 28(3):144–158. [PubMed: 17147056]
12. Korc M. Pancreatic cancer-associated stroma production. Am. J. Surg. Oct; 2007 194(4 Suppl):S84–6. [PubMed: 17903452]
13. D'Onofrio M, et al. Elastography of the pancreas. Eur. J. Radiol. Mar; 2014 83(3):415–419. [PubMed: 23726121]
14. Kawada N, et al. Potential use of point shear wave elastography for the pancreas: a single center prospective study. Eur. J. Radiol. Apr; 2014 83(4):620–4. [PubMed: 24445135]
15. Yashima Y, et al. Acoustic radiation force impulse elastography for noninvasive assessment of chronic pancreatitis. J. Gastroenterol. Apr; 2012 47(4):427–32. [PubMed: 22065162]

16. Harada N, et al. Acoustic radiation force impulse imaging of the pancreas for estimation of pathologic fibrosis and risk of postoperative pancreatic fistula. J. Am. Coll. Surg. Nov; 2014 219(5):887–894. e5. [PubMed: 25262282]
17. Park MK, Jo J, Kwon H, Cho JH, Oh JY. Usefulness of acoustic radiation force impulse elastography in the differential diagnosis of benign and malignant solid pancreatic lesions. Ultrasonography. Jan.2014 33:26–33. [PubMed: 24936492]
18. Wu T, Felmlee JP, Greenleaf JF, Riederer SJ, Ehman RL. Assessment of thermal tissue ablation with MR elastography. Magn. Reson. Med. Sep.2000 2001 45:80–87. [PubMed: 11146489]
19. Righetti R, Kallel F, Stafford R. Elastographic characterization of HIFU- induced lesions in canine livers. Ultrasound Med. Biol. 1999; 25(7):1099–1113. [PubMed: 10574342]
20. Xia R, Thittai AK. Real-time monitoring of high-intensity focused ultrasound treatment using axial strain and axial-shear strain elastograms. Ultrasound Med. Biol. Mar; 2014 40(3):485–95. [PubMed: 24361216]
21. Bercoff J, Pernot M, Tanter M, Fink M. Monitoring thermally-induced lesions with supersonic shear imaging. Ultrason. Imaging. 2004; 26(2):71–84. [PubMed: 15344412]
22. Arnal B, Pernot M, Tanter M. Monitoring of thermal therapy based on shear modulus changes: II. Shear wave imaging of thermal lesions. IEEE Trans. Ultrason. Ferroelectr. Freq. Control. Aug; 2011 58(8):1603–1611. [PubMed: 21859579]
23. Arnal B, Pernot M, Tanter M. Monitoring of thermal therapy based on shear modulus changes: I. shear wave thermometry. IEEE Trans. Ultrason. Ferroelectr. Freq. Control. Feb; 2011 58(2):369–378. [PubMed: 21342822]
24. Bing KF, Rouze NC, Palmeri ML, Rotemberg VM, Nightingale KR. Combined Ultrasonic Thermal Ablation with Interleaved ARFI Image Monitoring Using a Single Diagnostic Curvilinear Array: A Feasibility Study. Ultrason. Imaging. Oct; 2011 33(4):217–232. [PubMed: 22518953]
25. Lizzi FL, et al. Radiation-force technique to monitor lesions during ultrasonic therapy. Ultrasound Med. Biol. Nov; 2003 29(11):1593–1605. [PubMed: 14654155]
26. Curiel L, Huang Y, Vykhodtseva N, Hynynen K. Focused ultrasound treatment of VX2 tumors controlled by local harmonic motion. Phys. Med. Biol. Jun; 2009 54(11):3405–3419. [PubMed: 19436103]
27. Souchon R, et al. Visualisation of HIFU lesions using elastography of the human prostate in vivo: preliminary results. Ultrasound Med. Biol. Jul; 2003 29(7):1007–1015. [PubMed: 12878247]
28. Hou GY, Marquet F, Wang S, Apostolakis I-Z, Konofagou EE. High Intensity Focused Ultrasound Monitoring using Harmonic 1 Motion Imaging for Focused Ultrasound (HMIFU) under boiling or slow denaturation conditions. IEEE Trans. Ultrason. Ferroelectr. Freq. Control.
29. Hou G, et al. Sparse matrix beamforming and image reconstruction for real-time 2D HIFU monitoring using Harmonic Motion Imaging for Focused Ultrasound (HMIFU) with in vitro validation. IEEE Trans. Med. Imaging. Jun; 2014 33(11):2107–2117. [PubMed: 24960528]
30. Olive KP, Tuveson DA. The use of targeted mouse models for preclinical testing of novel cancer therapeutics. Clin. Cancer Res. Sep; 2006 12(18):5277–5287. [PubMed: 17000660]
31. Olive KP, et al. Inhibition of Hedgehog signaling enhances delivery of chemotherapy in a mouse model of pancreatic cancer. Science. Jun; 2009 324(5933):1457–1461. [PubMed: 19460966]
32. Choi JJ, Pernot M, Small SA, Konofagou EE. Noninvasive, transcranial and localized opening of the blood-brain barrier using focused ultrasound in mice. Ultrasound Med. Biol. 2007; 33(1):95–104. [PubMed: 17189051]
33. Luo J, Konofagou E. A fast normalized cross-correlation calculation method for motion estimation. IEEE Trans. Ultrason. Ferroelectr. Freq. Control. Jun; 2010 57(6):1347–1357. [PubMed: 20529710]
34. Konofagou EE, Hynynen K. Localized harmonic motion imaging: theory, simulations and experiments. Ultrasound Med. Biol. Oct; 2003 29(10):1405–1413. [PubMed: 14597337]
35. Vappou J, Maleke C, Konofagou EE. Quantitative viscoelastic parameters measured by harmonic motion imaging. Phys. Med. Biol. Jun; 2009 54(11):3579–3594. [PubMed: 19454785]
36. Konofagou EE, Ottensmeyer M, Agabian S, Dawson SL, Hynynen K. Estimating localized oscillatory tissue motion for assessment of the underlying mechanical modulus. Ultrasonics. Apr; 2004 42(1–9):951–956. [PubMed: 15047412]

37. Hou GY, Marquet F, Wang S, Konofagou EE. Multi-parametric monitoring and assessment of high-intensity focused ultrasound (HIFU) boiling by harmonic motion imaging for focused ultrasound (HMIFU): an ex vivo feasibility study. Phys. Med. Biol. Mar; 2014 59(5):1121–1145. [PubMed: 24556974]

38. Curiel L, Chopra R, Hynynen K. In vivo monitoring of focused ultrasound surgery using local harmonic motion. Ultrasound Med. Biol. Jan; 2009 35(1):65–78. [PubMed: 18805626]

39. Vappou J, Hou GY, Marquet F, Shahmirzadi D, Grondin J. method for measuring elastic properties of biological tissues using harmonic motion imaging (HMI) s. Phys. Med. Biol. 2015

40. Bussels B, et al. Respiration-induced movement of the upper abdominal organs: a pitfall for the three-dimensional conformal radiation treatment of pancreatic cancer. Radiother. Oncol. Jul; 2003 68(1):69–74. [PubMed: 12885454]

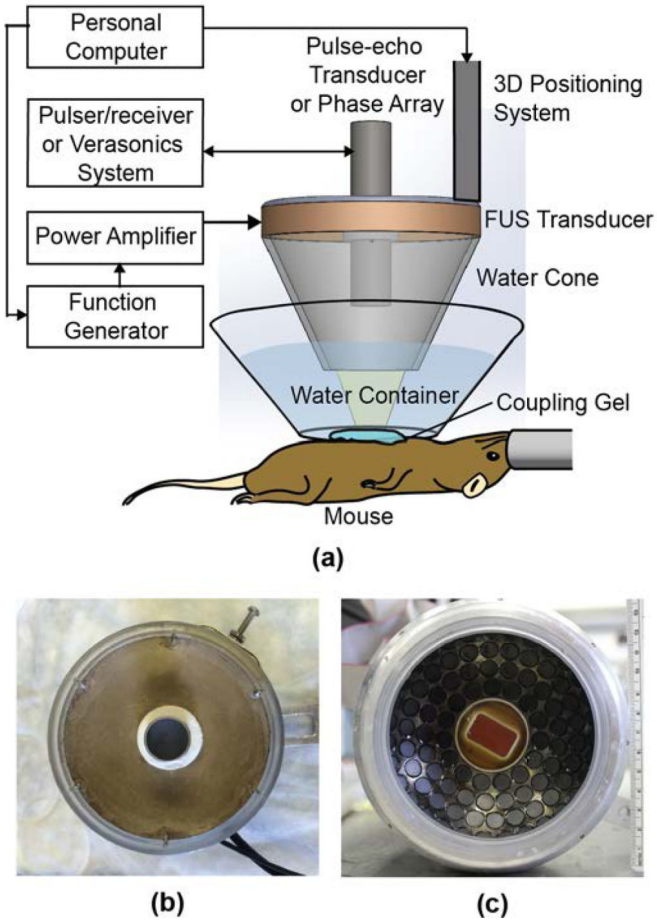

Fig. 1.

(a) Illustration of the experimental setup. (b) Picture of the 1D HMI transducer pair. (c) Picture of the 2D HMI transducer pair.

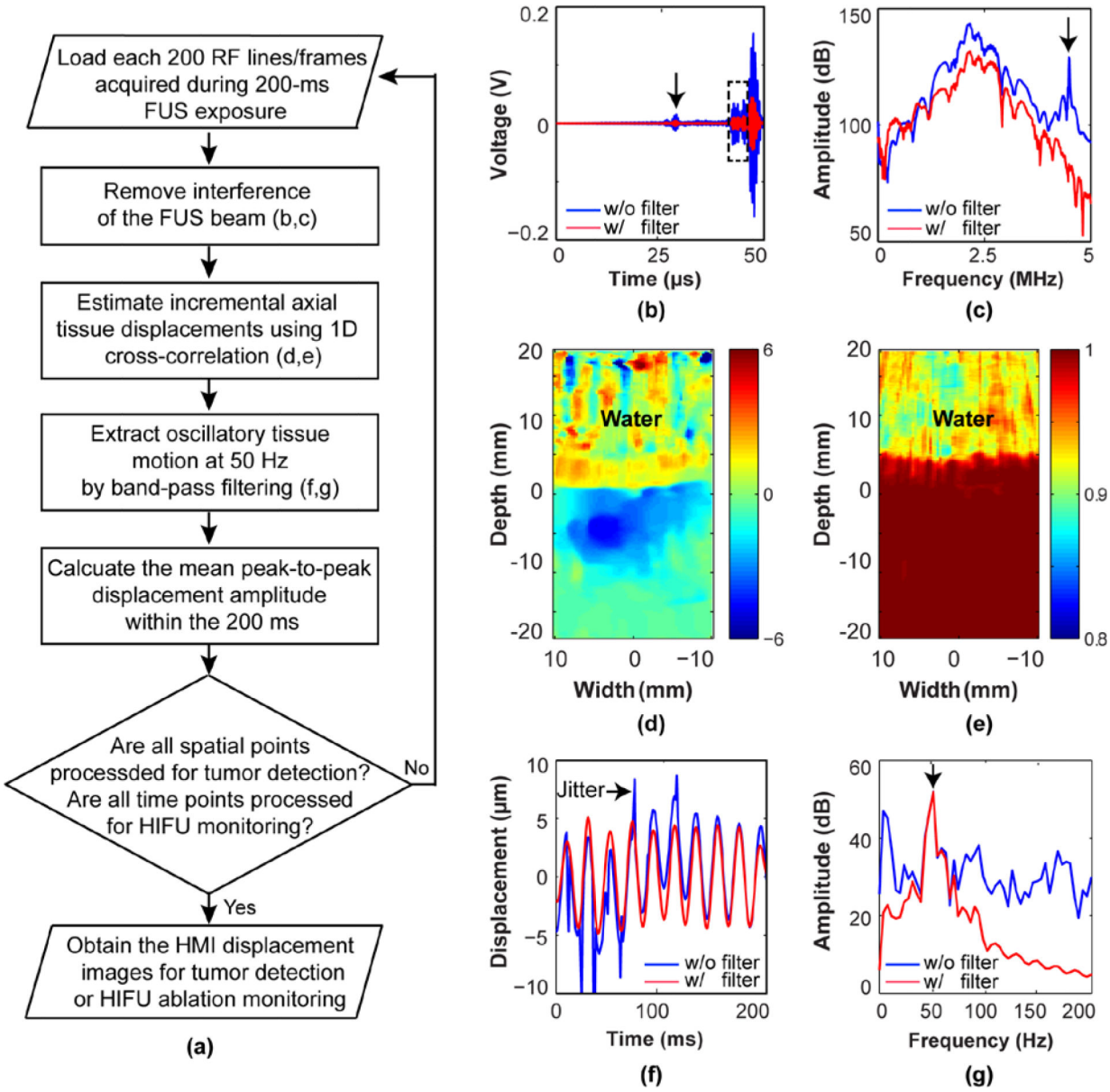

Fig. 2.

(a) Flow chart of HMI displacement estimation methods. Temporal (b) and spectral (c) plots of a RF signal before and after a low-pass filtering (f_{cutoff}=4 MHz) used to remove interference of the FUS beam. The arrow in (b) points to the ultrasound pulse reflected from the membrane at the bottom of the water cone connected with the FUS transducer. The rectangle highlights RF signal from the mouse. The arrow in (c) points to the center frequency of the FUS transducer at 4.5 MHz. (d) An example of the estimated incremental axial tissue displacement map using sequentially acquired tracking lines. (e) The corresponding correlation coefficient map. Temporal (f) and spectral (g) plots of tissue displacements before and after band-pass filtering with cutoff frequencies of f_{c1}=30 Hz and f_{c2}=70 Hz to extract oscillatory tissue motion at 50 Hz. The arrow in (f) points to high-level

jitter observed in the displacement estimation. The arrow in (g) points to the oscillatory tissue motion frequency at 50 Hz.

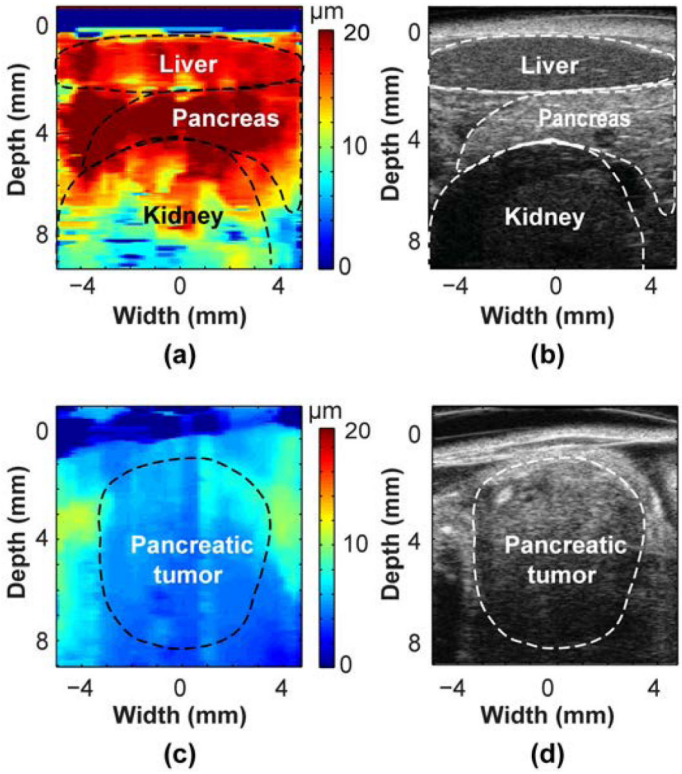

Fig. 3.

HMI images of (a) a normal pancreas and (c) a pancreas tumor. The corresponding Vevo B-mode images obtained at approximately the same scanning planes using a 30 MHz high-frequency probe are shown in (b) and (d), respectively. In (a), the location of the pancreas, as well as the liver and kidney in its close proximate, was outlined based on the corresponding Vevo B-mode image (b). In (c), the location of the pancreatic tumor was identified based on the corresponding Vevo B-mode image (d).

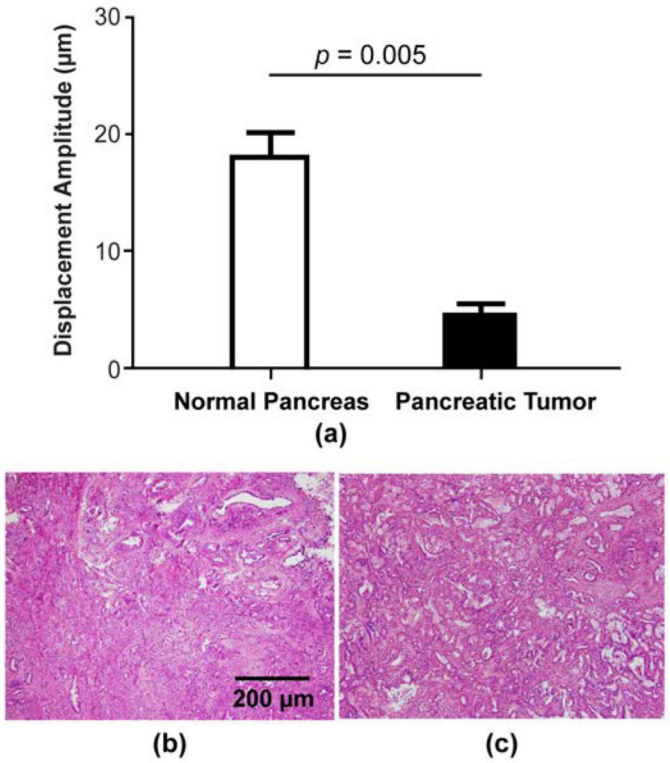

Fig. 4.

(a) Summary of peak-to-peak HMI displacements of normal pancreases in the wild-type mice and pancreatic tumors in the KPC mice. A statistically significant difference (p=0.005) in HMI displacement amplitudes was observed between the pancreatic tumors and normal pancreases. H&E stained images of pancreatic tumors without performing HMI (b) and after performing HMI (c) show no tissue damage was induced by HMI. The scale bar represents 200 μm.

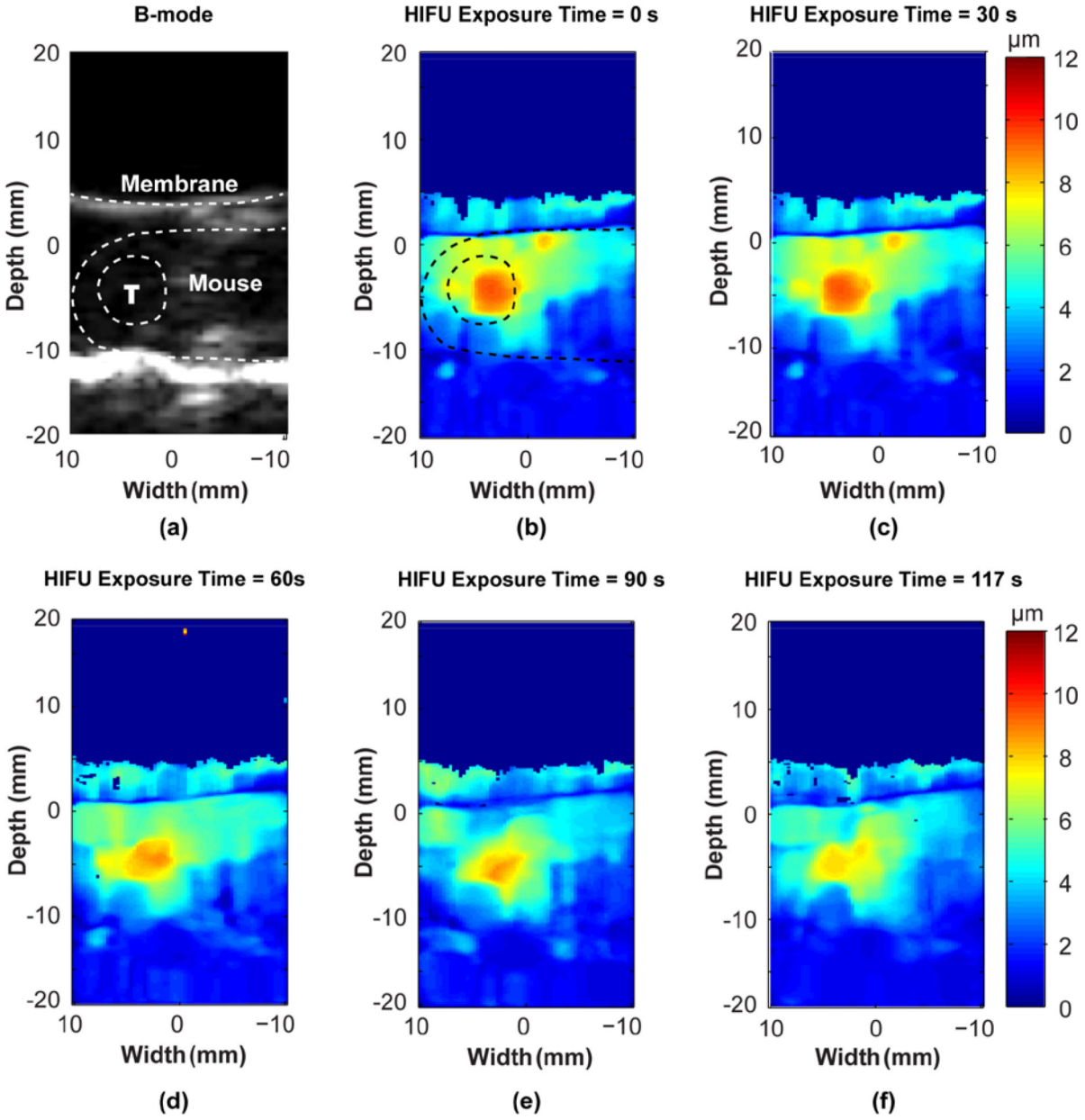

Fig. 5.

HMI monitoring of pancreatic tumor HIFU ablation. (b-f) peak-to-peak HMI displacement images at different HIFU exposure time points. (a) The corresponding B-mode image obtained at the same imaging plane using the same HMI probe before HIFU ablation. The locations of the membrane at the bottom of the water container, the mouse skin, and the tumor (labeled as “T”) are highlighted by dash lines. HIFU focal region, where the peak-to-peak HMI displacement was higher than all other regions, was precisely targeted within the tumor. The HMI displacements within the focal region decreased over time.

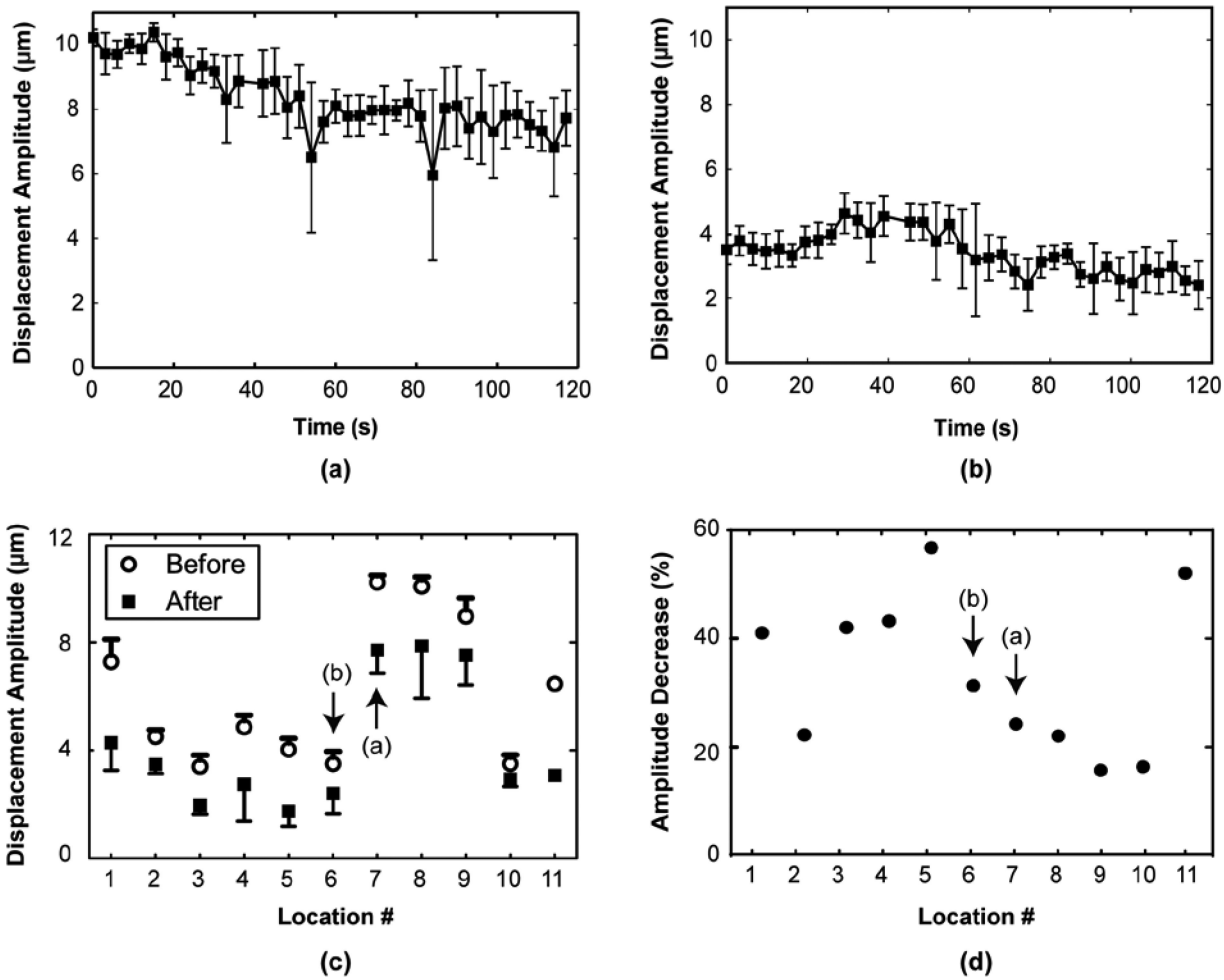

Fig. 6.

(a, b) Representative HMI displacement curves. Each curve shows the HMI displacement over the whole HIFU ablation process at the point with the highest displacement at t = 0 s. (a) HMI displacement curve for the case shown in Fig. 5. A trend of consistent reduction in HMI displacement amplitude was observed in (a) and a trend of displacement increase followed by decrease was observed in (b). (c) Summary of the mean and standard deviation of the peak-to-peak HMI displacements before and after HIFU ablation at 11 HIFU exposure locations. Signification difference (t-test, $p<0.05$) in the HMI displacement amplitude before and after HIFU ablation was observed in all locations. (d) Summary of the HMI displacement amplitude decrease percentages at the end of HIFU ablation (t=117 s) over the initial displacements at t = 0 s. In (c) ad (d), data points corresponding to the representative cases showed in (a) and (b) are labeled.

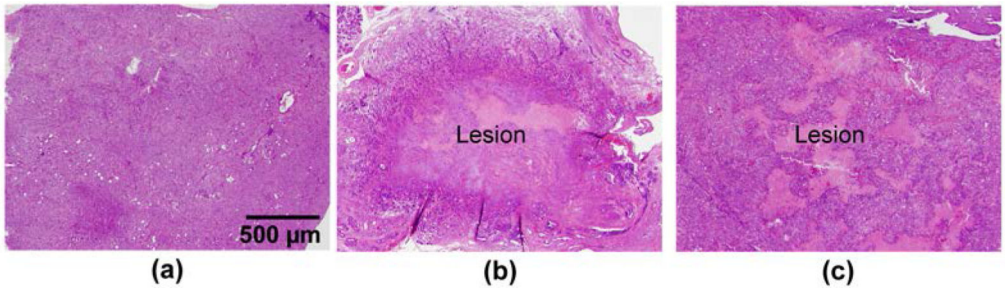

Fig. 7.

Representative H&E stained images of a pancreatic tumor without HIFU ablation (a) and two pancreatic tumors after HIFU ablation (b and c). Thermal lesions were observed in the latter two HIFU treated tumors. The scale bar represents 500 μm.

TABLE 1

PARAMETERS OF THE HMI SYSTEMS

	Parameters	**1D HMI system**	**2D HMI system**
FUS transducer	Type	Single element	93-element array
	Center frequency	4.755 MHz	4.5 MHz
	Duty cycle	100%	100%
	Acoustic power	5.04 W	7.56W
	Exposure time	200 ms	120 s
	Amplitude-modulation frequency	25 Hz	25 Hz
	Focal region size (Full-width at half maximum)	7 × 0.7 mm	1.7 × 0.4 mm
Imaging transducer	Type	Single element	64-element array
	Center frequency	7.5 MHz	2.5 MHz
	Sampling frequency	100 MHz	80 MHz
	PRF/ Frame rate	1 kHz	1 kHz